ES Mater. Manuf., 2020, **10**, 45-51

ES Materials and Manufacturing

DOI: https://dx.doi.org/10.30919/esmm5f939

Eosin-Y Sensitized Bi-layered ZnO Nanoflower-CeO_2 Photoanode for Dye-Sensitized Solar Cells Application

Suhail A.A.R. Sayyed,[1,2] Niyamat I. Beedri,[2] Pankaj K. Bhujbal,[2] Shoyebmohamad F. Shaikh[3] and Habib M. Pathan[2,*]

Abstract

The energy demand is increasing with the development of science and technology, as even common people are accessible to use different home appliances, devices, and gadgets. Solar energy could be one feasible solution to the present and future energy crisis. Amongst different types of solar cells, dye-sensitized solar cells (DSSCs) can cope up with the situation by providing a cost effective and environmentally suitable solution. In the present work, Eosin-Y sensitized bi-layered ZnO nanoflower-CeO_2 photoanode was synthesized for DSSCs. The compact ZnO nanoflower-CeO_2 layers were deposited by the dip coating and doctor blade method, respectively. From the X-ray powder diffraction (XRD) analyses, the structures of both ZnO and CeO_2 were confirmed with the nanocrystalline size of ~15 and ~10 nm, respectively by the Scherrer formula. Scanning electron microscope (SEM) confirmed the nanoflower morphology for ZnO (useful in dye adsorption and electron transfer) and porous, rough and spongy morphology for CeO_2 (useful for dye adsorption). The band gap values of ~3.2 and ~3.1 eV for ZnO and CeO_2, respectively, were calculated using UV-Visible data by the Tauc's plot. After the device fabrication, from the J-V characteristics, the solar cell parameters for best-performing cells were calculated as open-circuit voltage of ~460 mV, short circuit photocurrent density of ~0.4m A/cm^2 and a fill factor of ~55%.

Keywords: Dye sensitized solar cells; Photoanode; Nanoflower ZnO; CeO_2.
Received date: 16 August 2020; Accepted date: 18 November 2020.
Article type: Research article.

1. Introduction

With the increasing demand for energy worldwide, dye-sensitized solar cells (DSSCs) come to be a feasible, cost effective solution. DSSCs using ruthenium-based dyes have good efficiencies at the cost of the environmentally unsuitable and non-economical device. The solution is the low cost natural or organic dyes. But the efficiency of the devices using natural or organic dyes is less. There are mainly four components in a DSSC: wide band gap semiconductor, dye (or sensitizer), electrolyte, and counter electrode. Optimizing all these four components results in the best performance.

Various research groups are trying to implement different wide band gap materials for photoanode such as TiO_2,[1-3] ZnO,[4-6] SnO_2,[7-8] Nb_2O_5,[9-10] CeO_2,[11-13] MoO_3,[14] etc. One of the most important parameters is the conduction band position of the wide band gap material used and the lowest unoccupied molecular orbital (LUMO) level of the dye. For proper electron transfer, the LUMO level of the dye must be above the conduction band position of the wide band gap material used. In DSSCs, back reactions of electrons in the conduction band of a wide band gap material with dye and/or electrolyte molecules result in the loss of performance of the devices.

To avoid or suppress these losses, researchers are trying to use bi-layered materials such as TiO_2-CeO_2,[15-17] ZnO-CeO_2,[18] TiO_2-ZrO_2,[19] TiO_2-Nb_2O_5,[20] ZnO-Nb_2O_5,[21] *etc*. Also few researchers have used CeO_2 as a mirror-like structure for the scattering of light within the photoanode for a maximum absorption of incident photons along with TiO_2[17] and ZnO.[18] In the present work, we have used nanoflower ZnO and CeO_2 nanoparticles as compared with the mirror-like coating of CeO_2 used by H. Yu *et al.*[17] and Rai *et al.*[18]

In the present work, we have used a bi-layered ZnO nanoflower-CeO_2 photoanode. The nanoflower morphology of ZnO was used to increase the surface area for dye adsorption as well as to provide extra paths for electron transfer. The porous, rough, and spongy morphology of CeO_2 is useful for maximum adsorption of dye.

[1] *Department of Physics, B.P.H.E. Society's Ahmednagar College, Ahmednagar – 414 001, Maharashtra, India*
[2] *Advanced Physics Laboratory, Department of Physics, Savitribai Phule Pune University, Pune – 411007, Maharashtra, India*
[3] *Department of Chemistry, College of Science, King Saud University, Riyadh-11451, Saudi Arabia*
* *Email:* pathan@physics.unipune.ac.in *(Habib M. Pathan)*

2. Experimental section

2.1 Materials and Methods

Fluorine doped tin oxide (FTO) glass with a sheath resistance of 7 Ω/cm^2 was purchased from Macwin, India. The compact layer of the ZnO nanoflower structure on FTO was prepared using the dip coatings method. Zinc acetate and ammonium hydroxide were both purchased from Thomas baker along with doubled distilled water (DDW) were used for dip coating. A typical method of precipitation was used for the synthesis of CeO_2 nanoparticles using cerium nitrate ($Ce(NO_3)_3.6H_2O$, High Purity Laboratory Chemicals (HPLC)) and 20% NH_4OH (Thomas Baker) was used as precipitant. For making a paste, ethyl cellulose (HPLC) and terpineol (HPLC) were used along with ethyl alcohol. The Eosin-Y (HPLC) and ethyl alcohol were used for dye preparation. The electrolyte solution was prepared in solvent acetonitrile (Thomas Baker) by adding lithium iodide (Thomas Baker) and iodine resublimed (Kemphasol) for iodide/tri-iodide couple.

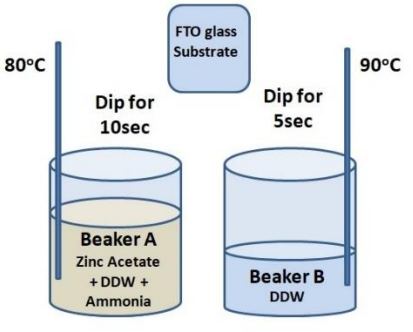

Fig. 1 Dip coatings of ZnO nanoflower.

2.2 Deposition of ZnO nanoflowers using dip coatings

There are various methods for the synthesis of ZnO.[22-25] For the synthesis of dip-coated ZnO nano-flowers,[24-25] two beakers were used (The process is shown in Fig. 1):

Beaker A: Zinc acetate solution of 0.05 M was prepared in DDW. This solution was slowly heated and when the temperature reached 40°C, 5 mL ammonia solution was added drop-wise. Initially, the precipitate was formed, later a clear solution was formed, then continuous ammonia solution was added to get precipitate and the temperature was maintained at 80°C. The pH of the solution was maintained in between 11.5 to 12.5.

Beaker B: 50 mL DDW. The temperature of this beaker was maintained at 90°C.

The substrates (FTO glasses) were cleaned with DDW, acetone, and ethyl alcohol. The substrate was dipped in Beaker A for 10 sec and Beaker B for 5sec to clean excess ions. This process was repeated for 25-30 cycles. A good adhesive film was obtained on the substrate. Then the substrate was cleaned in DDW and annealed at 300°C for one hour. Hence, the prepared films were characterized by various characterization techniques.

2.3 Synthesis of CeO_2 nanoparticles

For the preparation of nanocrystalline CeO_2 powder,[12-13,15,26-27] cerium nitrate solution in DDW was used as a source of Ce^{4+} ions. Ammonia solution was added to this solution as a source of OH^- ions. The obtained precipitant was $Ce(OH)_2$. This powder was annealed at 450°C to obtain CeO_2 powder, which was characterized by various characterization techniques.

2.4 Preparation of bi-layered photoanode and its sensitization

For making a uniform paste, 0.5 g synthesized CeO_2 powers was mixed with ethyl cellulose (0.4 g) and anhydrous terpineol (2.5 g). This mixture was then ground in mortar and pastle, and 5 mL ethanol was gradually added to get a jelly-like viscous uniform paste. Later by using the doctor-blade method, this paste was deposited on ZnO nanoflower coated FTO glass (prepared in Section 2.1). After drying for 1 hour, these photoanodes were annealed at 450°C for 1 hour. The dye solution (0.3 mM) was prepared by adding 19.437 mg of Eosin-Y dye (molecular weight=647.9) in 100 mL ethyl alcohol. Later, the photoanode was kept in the Eosin-Y dye solution. All these steps are shown in Fig. 2.

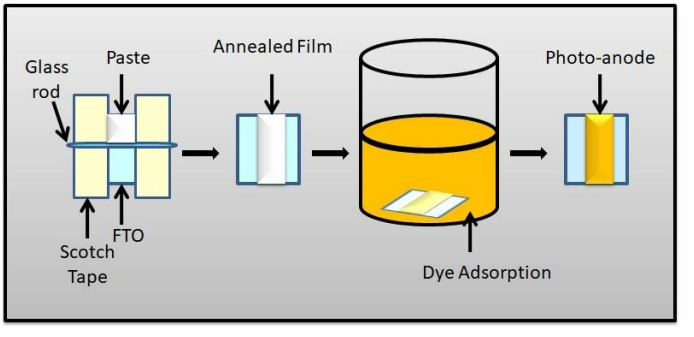

Fig. 2 Preparation of bi-layered photoanode and it's Sensitization.

2.5 Preparation of the electrolyte solution

The electrolyte solution was prepared by making a solution of 0.5 M LiI and 0.05 M I_2 in acetonitrile. This solution was mixed for 1 hour using a magnetic stirrer at room temperature.[13,28]

2.6 Preparation of counter electrode

Initially, all the contaminants from the surface of FTO glass were removed by cleaning with DDW, acetone, and ethanol. Then by using the flame of the candle, the lampblack was deposited on the conducting surface of FTO glass, which was used as a counter electrode.

2.7 Cell fabrication

To fabricate the final device, few drops of the above-prepared electrolyte (Section 2.5) were added to the Eosin-Y sensitized photoanode (Section 2.4). And then it was clamped with the counter electrode (Section 2.6) with the help of binder clips.

2.8 Characterizations

Various techniques were used for the characterization of the sample, dye, and DSSCs. The structures of both ZnO

nanoflower and nanocrystalline CeO_2 powder were characterized by XRD (Model No. D-8 Advance Bruker axs Germany, with a monochromator Cu Kα, λ = 1.54Å). The surface morphologies of ZnO nanoflower films and CeO_2 films were studied using SEM (Model No. JEOL–JSM 6360-A). The studies on diffused reflectance spectroscopy (DRS) for the absorption spectra of ZnO and CeO_2 were carried out by using the UV–Visible absorption spectrophotometer (Jasco Model: V-670). The absorption spectrum of the Eosin-Y dye was also studied by the same UV-Visible spectrophotometer in the range of 200 to 800 nm. The J-V characteristics of the cells were studied using Keithley Meter (Model 2400) with a 25 mW/cm^2 LED source.

3. Results and discussion

3.1 Characterization of ZnO nanoflower films

3.1.1 XRD analyses

From the XRD analyses, all the detected peaks confirmed the ZnO wurtzite structure (PDF code no: 00-036-1451).[29,30] We got peaks at angles 2θ=31.5, 33.6, 35.6, 46.8, 56.1, 62.2, 65.8, 67.4, 68.6, 72.1, 76.5°, corresponding to the (100), (002), (101), (102), (110), (103), (200), (112), (201), (004), (202) Miller planes, respectively (shown in Fig. 3). Using the Scherrer formula, the nanoparticle size was calculated as ~15 nm.

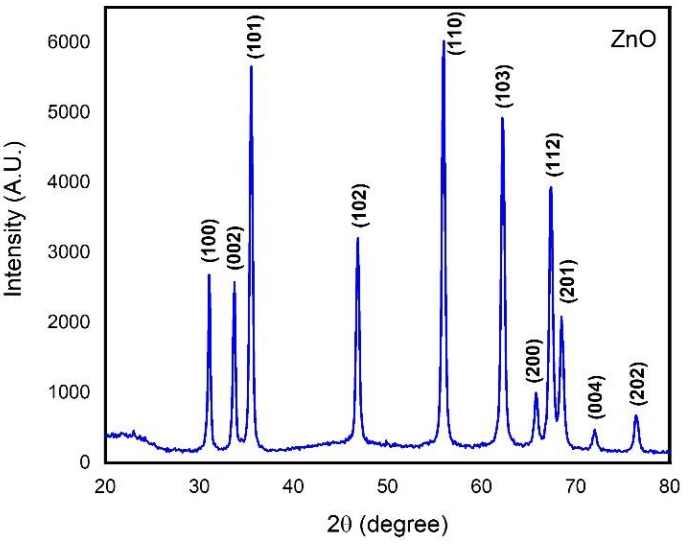

Fig. 3 XRD analyses of ZnO nanoflower film.

3.1.2 Scanning Electron Microscopy (SEM)

The SEM images of ZnO nanoflowers at different magnifications are shown in Fig. 4. The morphology of ZnO nanoflower is helpful for improving the performance of DSSCs in two ways. It increases the surface area, resulting in more dye adsorption and there is a drastic increase in the number of paths available for the electron transfer. Different researchers have implemented ZnO nanoflowers to exploit its extraordinary properties for improving the solar cell performance.[31]

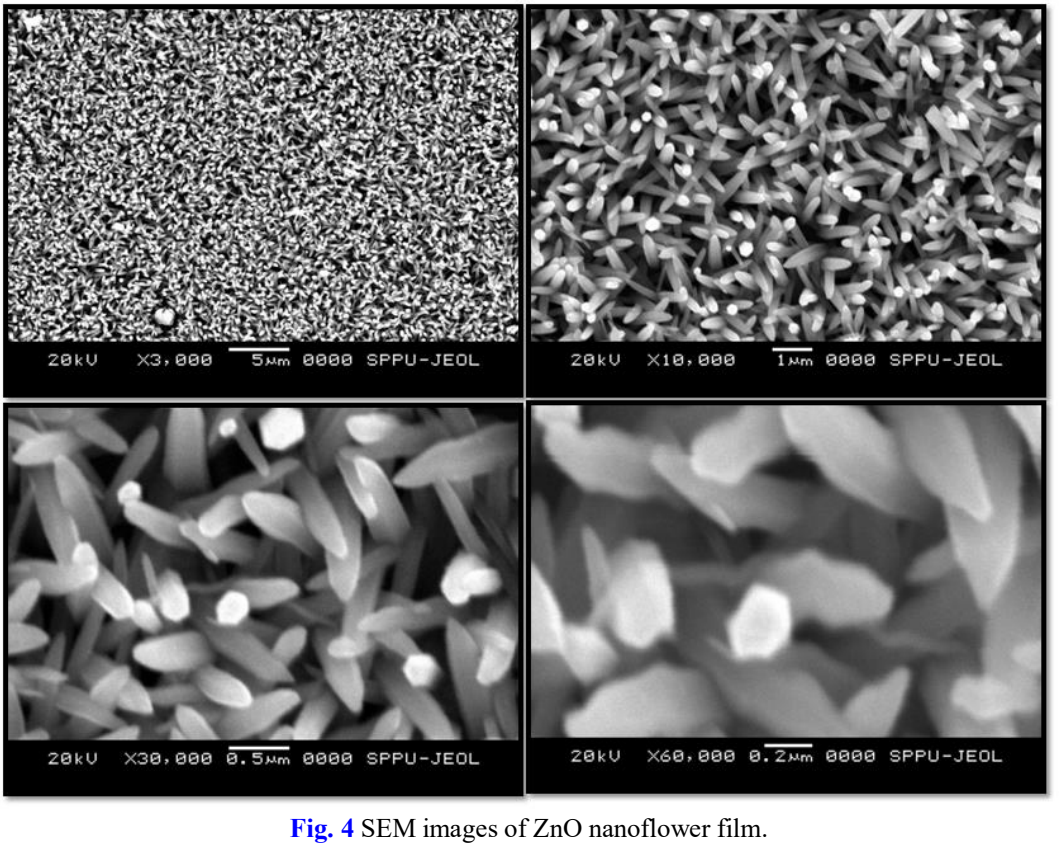

Fig. 4 SEM images of ZnO nanoflower film.

3.1.3 UV-visible spectra and band gap calculations

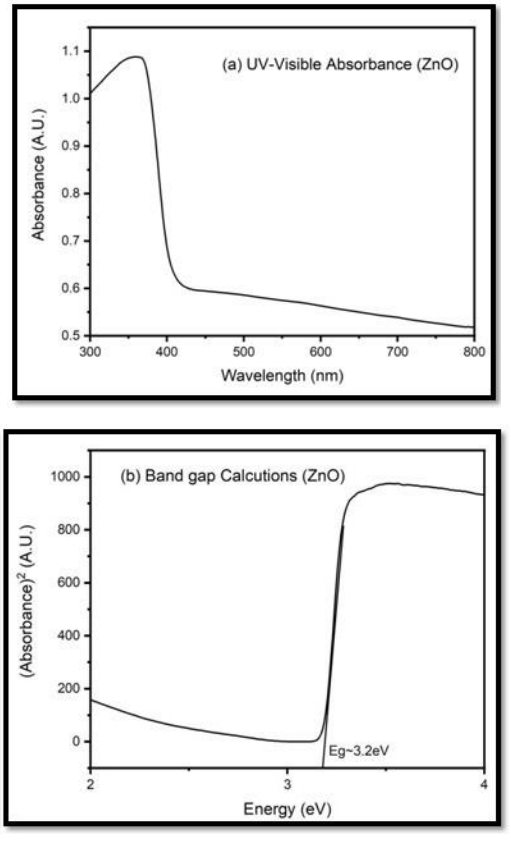

Fig. 5 (a) UV-Visible Absorption Spectra (ZnO) (b) Band gap Calculations (ZnO).

Fig. 5(a) shows the typical UV-visible absorption spectra of ZnO. The maximum absorption is at ~350nm. Fig. 5(b) shows the band gap calculations for the ZnO film using the Tauc's plot. The band gap of ZnO was found to be ~3.2 eV.

3.2. Characterization of CeO_2 nanopowder

3.2.1 XRD Analyses

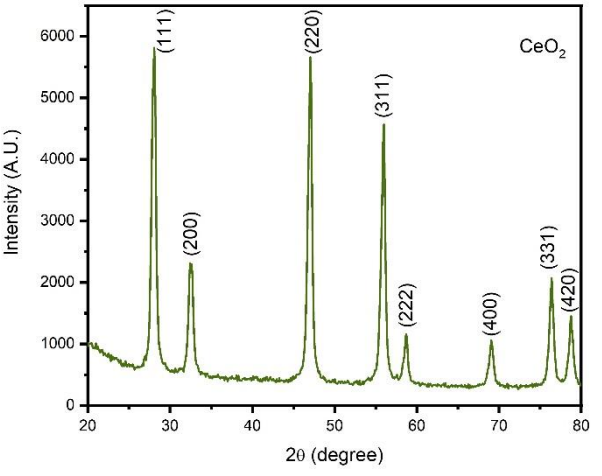

Fig. 6 XRD analyses of nanocrystalline CeO_2.

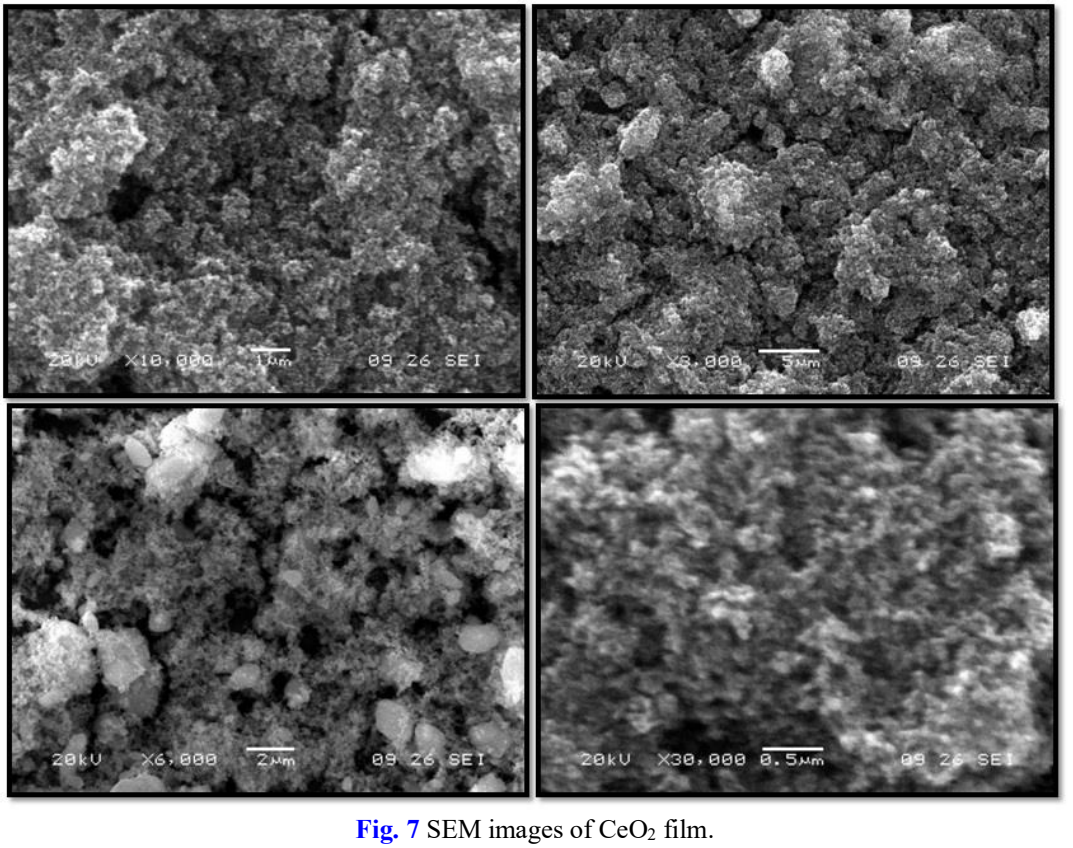

Fig. 7 SEM images of CeO_2 film.

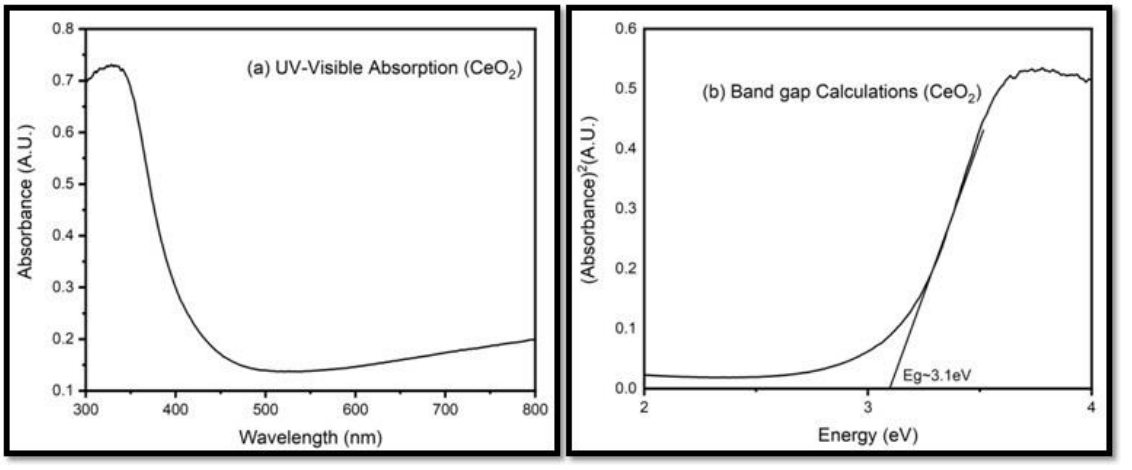

Fig. 8 (a) UV-Visible absorption spectra (CeO_2) and (b) band gap calculations (CeO_2).

The cubic structure of CeO_2 was confirmed from the XRD data shown in Fig. 6 ((JCPDS no. 81-0792, ICSD#072155, space group: Fm3m (225), unit cell parameters: a=b=c=5.4124 Å). The XRD peaks at angles 2θ= 28.5, 33.2, 47.4, 56.5, 59.2, 68.2, 76.7, and 79.2° correspond to the miller planes of (111), (200), (220), (311), (222), (400), (331), and (420), respectively.[12-13,15] The nanoparticle size of CeO_2 was ~10 nm calculated by the Scherrer formula.

3.2.2 Scanning electron microscopy (SEM)

Fig. 7 show the SEM images of CeO_2 photoanode at different magnifications. The surface morphology is porous, rough, and spongy. This type of surface morphology is useful for maximum dye adsorption.

3.2.3 UV-visible spectra and band gap calculations

Fig. 8(a) shows the UV-Visible absorption spectra of CeO_2. The peak occures at ~380 nm. From Fig. 8(b), the band gap of CeO_2 was calculated as 3.1 eV. As we go towards nano-size for most of the materials, due to the quantum size effect, there is an increase in the band gap. But in CeO_2, due to the presence of oxygen vacancies, as we go towards nano-size, there is decerease in the band gap.[32]

3.3. Characterization of Eosin-Y dye

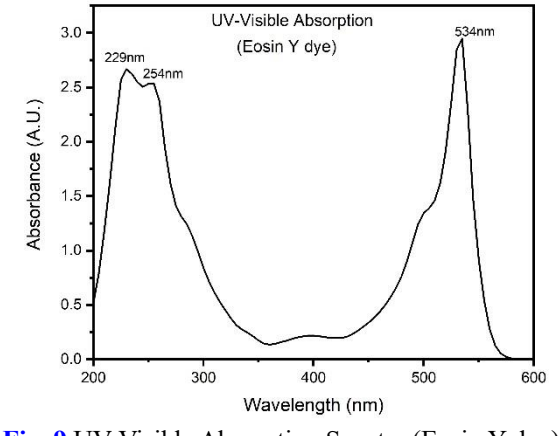

Fig. 9 UV-Visible Absorption Spectra (Eosin Y dye).

Fig. 9 shows the UV-visible absorption spectra of Eosin-Y dye. Here three peaks at 229, 254, and 534 nm are observed. Also, there is a good absorption of visible light in the range of 400 to 600 nm. The LUMO level of Eosin-Y dye is above the conduction band of CeO_2, which is helpful for fast electron transfer from the LUMO level to the conduction band of CeO_2 and then further into conduction band of ZnO.[6-8,13]

3.4 Cell testing

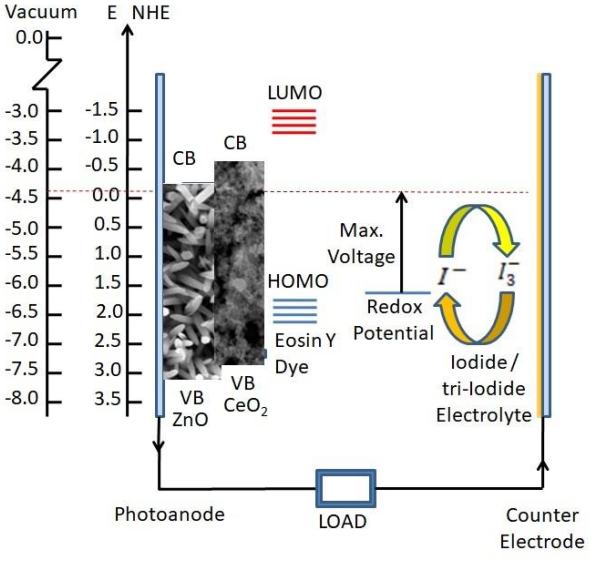

Fig. 10 Schematic of Eosin-Y sensitized bi-layered ZnO nanoflower-CeO_2 photoanode.

The schematic of Eosin-Y dye-sensitized bi-layered ZnO nanoflower-CeO_2 photoanode is shown in Fig. 10. Due to the use of the ZnO nanoflower structure, there is a drastic increase in the surface to volume ratio, resulting in a large increase in the number of paths for electron transfer. The nanoflower helps in adsorbing more quantity of dye. The porous structure formed using nano-sized CeO_2 is useful in adsorbing more quantity of dye with the increased surface area.

One of the major issues limiting the performance in DSSCs is the back reactions of electrons from conduction band of photoanode with dye and/or electrolyte molecules. The

conduction band position of CeO_2 is below LUMO level of Eosin-Y dye and above the conduction band of ZnO. This results in a fast electron transfer from Eosin-Y dye to the conduction band of CeO_2, and further to the conduction band of ZnO. This type of the fabricated device helps to reduce the back reactions of electrons with dye and/or electrolyte molecules. A similar methodology was applied by different researchers by implementing a bi-layered photoanode for an improved performance of DSSCs.[15-21]

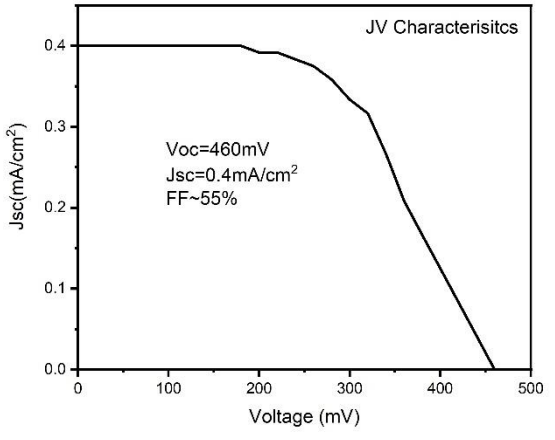

Fig. 11 J-V characteristics of Eosin-Y sensitized bi-layered ZnO nanoflower-CeO_2 photoanode.

Fig. 11 shows the J-V characteristics of Eosin-Y dye-sensitized bi-layered ZnO nanoflower-CeO_2 photoanode based DSSC. Open-circuit voltage (V_{oc}) ~460 mV, short circuit photocurrent density (J_{sc}) ~0.4 mA/cm^2 with fill factor (FF) ~55% were obtained together with an efficiency ~0.01% under low light condition (1 mW/cm^2).

4. Conclusion

In conclusion, bi-layered ZnO nanoflower-CeO_2 photoanode was successfully synthesized. The crystalline size of ZnO and CeO_2 were measured as ~15 and ~10 nm, respectively. Nanoflower structure of ZnO (confirmed by SEM images) is useful for dye adsorption as well as electron transfer by providing extra paths for electrons. The porous, rough, and spongy structure of CeO_2 (confirmed by SEM images) is useful for dye adsorption. The band gap calculated from UV-Visible data for ZnO and CeO_2 is 3.2 and 3.1 eV, respectively. From the UV-Visible absorption spectra of Eosin-Y dye, it is sure that it captures a long-range of visible light photons. The conduction band of CeO_2 is below the LUMO level of Eosin-Y dye and above the conduction band of ZnO. This helps to enhance the performance of the cell by reducing the back reactions of electrons with the dye and/or the electrolyte molecules. These solar cells show an open circuit voltage (V_{oc}) ~460 mV, short circuit photocurrent density (J_{sc}) ~0.4 mA/cm^2 together with FF of ~55%.

Acknowledgments

Dr. Suhail A. A. R. Sayyed is thankful to Hon. Principal Dr. R. J. Barnabas, B.P.H.E. Society's Ahmednagar College, Ahmednagar for kind support and constant motivation.

Conflict of Interest

The authors declare no competing financial interests.

Supporting Information

Not applicable

References

[1] B. O'Regan and M. Grätzel, *Nature*, 1991, **353**, 737–740, doi: 10.1038/353737a0.

[2]V. Shanmugam, S. Manoharan, S. Anandan and R. Murugan, *Spectrochim. Acta - Part A Mol. Biomol. Spectrosc.*, 2013, **104**, 35–40, doi: 10.1016/j.saa.2012.11.098.

[3] A. S. Shikoh, Z. Ahmad, F. Touati, R. A. Shakoor and S. A. Al-Muhtaseb, *Ceram. Int.*, 2017, **43**, 10540–10545, doi: 10.1016/j.ceramint.2017.05.113.

[4] W.-C. Chang, Y.-Y. Cheng, W.-C. Yu, Y.-C. Yao, C.-H. Lee and H.-H. Ko, *Nanoscale Res. Lett.*, 2012, **7**, 166, doi: 10.1186/1556-276X-7-166.

[5] S. S. Khadtare, A. P. Ware, S. Salunke-Gawali, S. R. Jadkar, S. S. Pingale and H. M. Pathan, *RSC Adv.*, 2015, **5**, 17647–17652, doi: 10.1039/C4RA14620D.

[6] S. S. Khadtare, S. R. Jadkar, K. N. Hui, R. S. Mane and H. M. Pathan, in 2014 International Renewable and Sustainable Energy Conference (IRSEC), *IEEE*, 2014, pp. 97–99**.** doi: 10.1109/IR-SEC.2014.7059876.

[7] S. Arote, R. Ingle, V. Tabhane and H. Pathan, *J. Renew. Sustain. Energy*, 2014, **6**, 013132, doi: 10.1063/1.4863692.

[8] A. B. F. Martinson, J. W. Elam, J. T. Hupp and M. J. Pellin, *Nano Lett.,* 2007, **7**, 2183–2187, doi: 10.1021/nl070160+.

[9] R. Panetta, A. Latini, I. Pettiti and C. Cavallo, *Mater. Chem. Phys.*, 2017, **202**, 289–301, doi: 10.1016/j.matchemphys.2017.09.030.

[10] N. I. Beedri, S. A. A. R. Sayyed, S. R. Jadkar and H. M. Pathan, in *AIP Conference Proceedings*, 2017, vol. 1832, doi.org/10.1063/1.4980224.

[11] A. Turkovic, *Sol. Energy Mater. Sol. Cells*, 1997, **45**, 275–281, doi: 10.1016/S0927-0248(96)00076-1.

[12] S. A. A R Sayyed, N. I. Beedri, V. S. Kadam And H. M. Pathan, *Bull. Mater. Sci.*, 2016, **39**, 1381–1387, doi: 10.1007/s12034-016-1279-7.

[13] S. A. A. R. Sayyed, N. I. Beedri and H. M. Pathan, *J. Mater. Sci. Mater. Electron.*, 2017, **28**, 5075–5081, doi:10.1007/s13204-015-0495-6.

[14] J. Theerthagiri, R. A. Senthil, M. H. Buraidah, J. Madhavan and A. K. Arof, *J. Mater. Sci. Technol.*, 2016, **32**, 1339–1344, doi: 10.1016/j.jmst.2016.03.003.

[15] S. A. A. R. Sayyed, N. I. Beedri, V. S. Kadam and H. M. Pathan, *Appl. Nanosci.*, 2016, **6**, 875–881, doi: 10.1007/s13204-015-0495-6.

[16] M. Tripathi and P. Chawla, *Ionics (Kiel).*, 2015, **21**, 541–546, doi: 10.1007/s11581-014-1172-6.

[17] H. Yu, Y. Bai, X. Zong, F. Tang, G. Q. M. Lu and L. Wang, *Chem. Commun.*, 2012, **48**, 7386–7388, doi: 10.1039/C2CC32239K.
[18] P. Rai, R. Khan, K.-J. Ko, J.-H. Lee and Y.-T. Yu, *J. Mater. Sci. Mater. Electron.*, 2014, **25**, 2872–2877, doi: 10.1007/s10854-014-1954-7.
[19] A. Kitiyanan and S. Yoshikawa, *Mater. Lett.*, 2005, **59**, 4038–4040, doi: 10.1016/j.matlet.2005.07.080.
[20] E. Barea, X. Xu, V. González-Pedro, T. Ripollés-Sanchis, F. Fabregat-Santiago and J. Bisquert, *Energy Environ. Sci.*, 2011, **4**, 3414, doi: 10.1039/C1EE01193F.
[21] N. I. Beedri, P. K. Baviskar, S. Jadkar and H. M. Pathan, *Int. J. of Modern Physics B,* 2018, **32**, 1840046, doi: 10.1142/S0217979218400465.
[22] N. I. Beedri, Y. A. Inamdar, S. A. A. R. Sayyed, A. V. Shaikh, S. R. Jadkar and H. M. Pathan, *Adv. Sci. Lett.*, 2014, **20**, 1147–1150, doi: 10.1166/asl.2014.5500.
[23] N. Beedri, Y. Inamdar, S. A. A. R. Sayyed, A. Shaikh, S. Jadkar and H. Pathan, *Chem. Chem. Technol.*, 2014, **8**, 283–286, doi: 10.23939/chcht08.03.283
[24] J. N. Hasnidawani, H. N. Azlina, H. Norita, N. N. Bonnia, S. Ratim and E. S. Ali, *Procedia Chem.*, 2016, **19**, 211–216, doi: 10.1016/j.proche.2016.03.095.
[25] A. Nagar, A. Kumar, S. Parveen, A. Kumar, H. Dhasmana, S. Husain, A. Verma and V. K. Jain, *Mater. Today Proc.*, doi: 10.1016/j.matpr.2020.02.087.
[26] M. J. Godinho, R. F. Gonçalves, L. P. S Santos, J. A. Varela, E. Longo and E. R. Leite, *Mater. Lett.*, 2007, **61**, 1904–1907, doi: 10.1016/j.matlet.2006.07.152.
[27] L. Y. Y. H. Liu, J. C. Zuo, X. F. Ren, *METALURGIJA*, 2014, **53**, 463–465.
[28] S. S. Khadtare, S. R. Jadkar, S. Salunke-Gawali and H. M. Pathan, *J. Nano Res.*, 2013, **24**, 140–145, doi: 10.4028/www.scientific.net/JNanoR.24.140.
[29] A. Khorsand Zak, Razali, W. H. B. Abd Majid and M. Darroudi, *Int. J. Nanomedicine*, 2011, 1399, doi: 10.2147/IJN.S19693.
[30] M. B. Bouzourâa, A. E. Naciri, A. Moadhen, H. Rinnert, M. Guendouz, Y. Battie, A. Chaillou, M.-A. Zaïbi and M. Oueslati, *Mater. Chem. Phys.*, 2016, **175**, 233–240, doi: 10.1016/j.matchemphys.2016.03.026.
[31] F. Xu and L. Sun, *Energy Environ. Sci.*, 2011, **4**, 818–841, doi: 10.1039/C0EE00448K.
[32] A. Corma, P. Atienzar, H. García and J.-Y. Chane-Ching, *Nat. Mater.*, 2004, **3**, 394–397, doi: 10.1038/nmat1129.